31st Annual International Conference of the IEEE EMBS
Minneapolis, Minnesota, USA, September 2-6, 2009

An *in vitro* System for Modeling Brain Reactive Responses and Changes in Neuroprosthetic Device Impedance

John P. Frampton, Mathew R. Hynd, Aytekin Vargun, Badri Roysam and William Shain, *Member, IEEE*

***Abstract*—Currently available methods for analyzing the structural properties of neural tissue are limited by the frequency at which data can be collected and by the need to sacrifice the specimen to correlate histology with other data. Electrical impedance spectroscopy (EIS) can be used to complement conventional histological and imaging-based methods by measuring real-time electrical data that can be ascribed to changes in tissue composition and structure. This report describes an impedance-based method for the analysis and modeling of the electrical properties of three-dimensional neural tissue constructs *in vitro*. This model system was used to assess the effects of cell density, type and organization on neuroprosthetic device electrode performance.**

I. Introduction

Chronic integration of microfabricated neuroprosthetic devices is currently limited by the ability to form stable interfaces with the central nervous system [12, 19]. It has been hypothesized that one mechanism underlying inconsistent device performance is the development of reactive cell and tissue responses after device implantation [20]. Unfortunately, few tools are available that permit real-time assessment of reactive response development and the impact on device electrical performance.

Electrochemical impedance spectroscopy (EIS) has been proposed as a method for evaluating the electrical properties of tissue surrounding devices [24]. EIS provides a method for the real time acquisition of electrical data that can be used to evaluate the composition and structure of neural tissue. It can be used in combination with neural recordings and histological data to describe how device performance can be affected by changes in tissue organization.

Impedance measurements are acquired by applying an AC potential to a working (device) electrode, and measuring the current response signal across the electrochemical system by way of a counter electrode and a stable, low impedance reference electrode [2, 8].

Biological materials exhibit electrical properties (resistive and capacitive elements) that can be measured using EIS. For instance, in brain tissue the extracellular matrix can impede the flow of current due to its protein- and proteoglycan-rich composition [24, 10]. In addition, densely packed cells contribute to tissue resistance by decreasing the amount of extracellular space (ECS) through which current passes. Individual cells also contribute a variety of circuit elements. Lipid bilayers can behave like capacitive elements and membrane channels can act as resistive elements [16, 9]. The formation of direct interactions (junctional complexes) between cells can also contribute resistance [5].

EIS is sensitive enough to detect monolayers of cells as well as deposited proteins/lipids[17]. EIS has even been used as a method for real-time cell tomography [11]. More recently, EIS has been used to monitor the brain responses to implanted neuroprosthetic devices [24]. These brain reactive responses involve a variety of cell types and involve time-dependent changes in tissue organization, ultimately resulting in the formation of electrically insulating glial sheaths around devices. Changes in impedance spectra were correlated with the extent of glial fibrillary acidic protein immunohistochemical signal around implant sites in rats [24].

This report describes an impedance based system for modeling the electrical properties of 3-D neural tissue cultures surrounding neuroprosthetic devices. These methods allow cell seeding conditions around electrodes to be modified by cell type and number, impedance measurements to be made over time, and modeling of the corresponding impedance spectra. In addition, automated image analysis and object feature association can be used to describe the localization of cells around device electrodes. Together these techniques can be used to assess the effects of glial cells on impedance measured from device electrodes and help develop strategies for improving device designs and tissue integration.

II. Methods

A. Impedance Measurement System

Devices were purchased from NeuroNexus Technologies (Ann Arbor MI). The NeuroNexus acute probe design

Manuscript received April 23, 2009. This work was supported in part by the Nanobiotechnology Center (NBTC) an STC program of the NSF under agreement number ECS-9876771, and by the NIBIB-supported Center for Neural Communication Technology (CNCT) P41-002030, R01NS044287 and R01EB005157.

John P. Frampton is a graduate student in the Department of Biomedical Sciences at the School of Public Health, State University of New York at Albany, Albany, NY 12222 USA (phone: 518-473-3629; fax: 518-474-3439; e-mail: jf7674@ albany.edu).

Matthew R. Hynd and William Shain are part of the Wadsworth Center (NYS DOH) and are faculty in the Department of Biomedical Sciences at the School of Public Health, State University of New York at Albany, Albany, NY 12222 USA (e-mail: shain@wadsworth,org).

Aytekin Vargun and Badri Roysam are at Rensselaer Polytechnic Institute, Troy, NY 12180 USA (e-mail:roysam@ecse.rpi.edu).

consisted of a 100 µm-wide silicon shank that was 3 mm in length and tapered to a point. Deposition of electrode materials and insulation layers were achieved through photolithographic processes. Electrodes were composed of iridium oxide, a material commonly used in stimulating electrodes due to its charge storage properties [23]. Electrodes were arranged in a 1x16 configuration along the silicon shank with a center-to-center spacing of 100 µm. Electrode area was 177 um^2.

Custom made chambers were designed to permit impedance measurement from recording devices and 3-D cell cultures. Culture chambers were fabricated around the prepackaged probe and PCB as described previously [6].

Impedance measurements were recorded using a Gamry potentiostat (Gamry, Warminster, PA). Impedance spectra were logarithmically decremented between 10 Hz and 100 kHz, at a constant 50 mV AC voltage. During recording sessions devices were placed in a Faraday cage to reduce electronic noise. An Ag/AgCl columnar electrode, filled with 2M KCl and sealed with a Vycor tip was used as a reference electrode. Individual device electrodes were connected to the working lead of the potentiostat using a customized 16-prong adapter. Platinum foil (2 cm long, 3 mm wide) was used as a counter electrode. HEPES-buffered Hanks' saline (HBHS) was used as a recording medium for all experiments.

A. Neural Tissue Constructs and Imaging

Cultures of primary glial cells were obtained following a previously described cell isolation procedure [1]. All procedures involving animals were approved by the Wadsworth Center IACUC. GGGGRGDY-functionalized alginate (0.5% wt/v) was used as a cell encapsulation material. 3-D neural tissue constructs were formed using a micromolding process [6]. Constructs were modified in terms of cell density (0-100,000 cells/µL) and cell type (LRM55 glial cells and mixtures of astrocytes and microglia), thus providing control over the tissue composition surrounding electrodes. Confocal microscopy was used to collect images from 3-D cultures labeled with either Syto40 or Hoechst 33342 nuclear stains in order to demonstrate the 3-D distribution of glia.

B. Impedance Modeling and Image Analysis

Impedance spectra, displayed as Bode and Nyquist plots, were fitted to equivalent circuits using a simplex non-linear least squares algorithm and Gamry Echem Analyst software (Fig. 1). Data from bare and cell-coated electrodes were fitted to equivalent circuit models represented by the solution resistance of the HBHS (R_{sol}), the charge transfer resistance of the electrode (R_{ct}), a constant phase element for the double layer capacitance (CPE), the capacitance contributed by cell plasma membranes (C_{cells}), and the porous bounded Warburg impedance used to model diffusion limitations in the system ($Z_{Warburg}$). Values for R_{sol} and CPE were fixed with respect to the bare electrode measurements, thus permitting accurate fitting of the remaining parameters. R_{ct} was not fixed due to the relatively large variations observed during measurement and possible interrelation with diffusion controlled processes.

Confocal images were analyzed using FARSIGHT software to extract object features and determine the spatial distribution of cell nuclei relative to the electrodes [4].

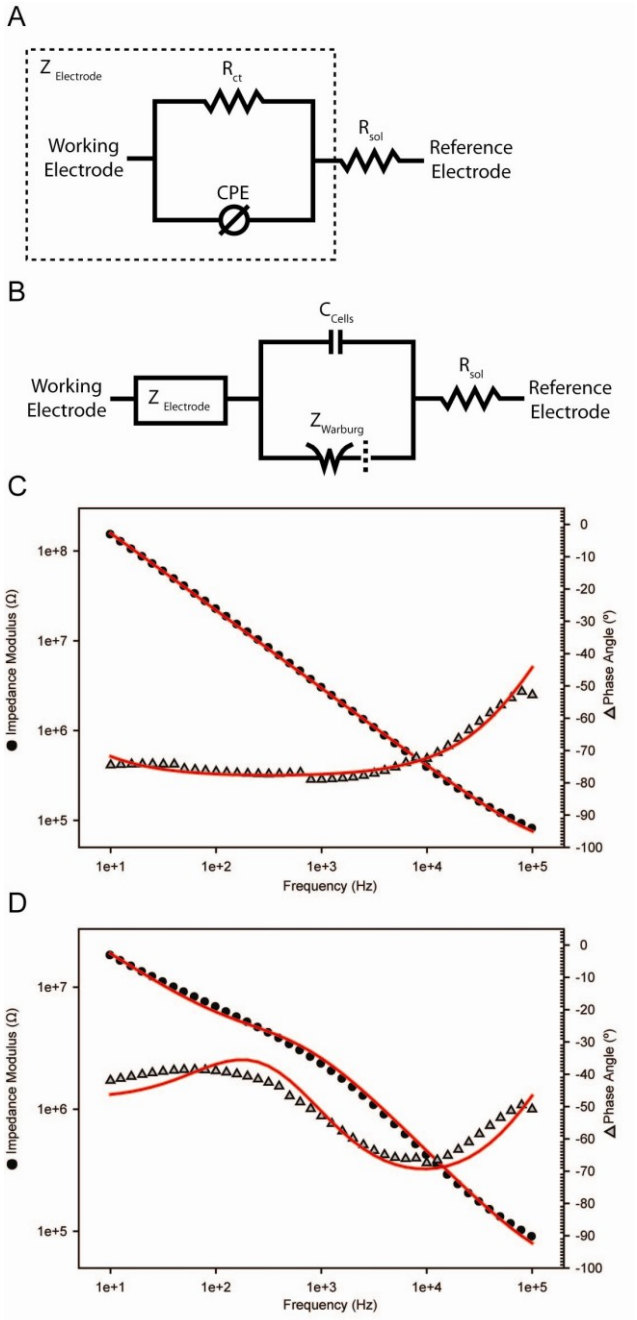

Fig. 1. Equivalent circuit modeling of electrodes coated with 3-D constructs. The proposed circuit model for bare electrodes is depicted in (A). The proposed circuit model for cell-coated electrodes (B) contains several additional elements including a Warburg element $Z_{Warburg}$ to model the resistance resulting from restriction of pathways for ionic species to diffuse through the ECS. An additional capacitive element was used to model the capacitance contributed by cell lipid bilayers. The fitted spectra are shown for an uncoated iridium electrode (C) and the same electrode after 3 days of cell culture within a high cell density glial construct (D). Black circles represent impedance modulus, grey triangles represent impedance phase, and red traces represent the corresponding fits.

Graphical representations, graph query tools, and 3-D rendering software were used to describe and display the spatial associations between cells and electrodes.

III. Results

Impedance spectra could be displayed as Bode plots (log impedance modulus and phase on the *y*-axes and log frequency on the *x*-axis). The average impedance modulus for iridium electrodes was 1.678 kΩ at 1 kHz. Iridium electrodes were capacitive in nature, as evidenced by the phase angle value over nearly all frequencies (-74.6° at 1 kHz for iridium; -90° indicates pure capacitance). This was confirmed by the slope of Nyquist plots (not shown), giving the ratio of resistance to –reactance (0.27 at 1 kHz, indicating a greater contribution from capacitance).

Electrode impedance values were within ranges reported in literature for microelectrodes of the materials used [7, 14, 21]. Net inductance was not observed in any recorded impedance spectra. Broken connections (impedance >10 MΩ at 1 kHz) were occasionally observed, and any affected electrodes were excluded from analysis.

Data from both bare electrodes and cell-coated electrodes could be accurately fitted to the equivalent circuits depicted in Fig. 1A. Average values for equivalent circuit parameters and goodness of fit (χ^2) for bare electrodes are displayed in Table I and were in agreement with initial estimates and previously reported findings [7, 23].

TABLE I
Equivalent Circuit Values

Electrode Type	Electrode Type
Iridium 177um^2	Iridium 177um^2 + cells
R_{sol}	R_{sol}
4.32 x 10^4 Ω	4.32 x 10^4 Ω
R_{ct}	R_{ct}
1.37x 10^9 Ω	4.03 x 10^6 Ω
CPE Y_0	CPE Y_0
1.68 x 10^{-10} Ssec^a	1.68 x 10^{-10} Ssec^a
CPE a	CPE a
8.70 x 10^{-1}	8.70 x 10^{-1}
	Warburg Y_0
	6.09 x 10^9 Ssec$^{(1/2)}$
	Warburg B
	3.79 x 10^4 sec$^{(1/2)}$
	C_{cells}
	2.74 x 10^{-10} F
Goodness of Fit	Goodness of Fit
1.98 x 10^{-3}	9.55 x 10^{-3}

Cell-seeded alginate constructs were established within chamber assemblies surrounding electrodes using the previously described process [6]. EIS data obtained from high cell density (100,000 cells/μL) cultures of LRM55 astroglia were used to develop an equivalent circuit model for the electrical components of cell-seeded alginate constructs. The equivalent circuit model for cell-seeded alginate constructs consisted of the model for uncoated electrodes with several additional circuit elements, where C_{cells} represents the capacitance contributed by cell plasma membranes and $Z_{Warburg}$ represents the porous bounded Warburg impedance used to model diffusion limitations in the system. Table I lists the values for the equivalent circuit parameters for iridium oxide electrodes before and after application of cells (spectra and fits shown in Fig. 1B,C). The curve fitting routine for both bare and cell coated electrodes converged in less than 50 iterations for all spectra sampled. These results demonstrate that EIS data from bare electrodes and electrodes surrounded by cells can be interpreted in terms of defined circuit elements.

FARSIGHT analysis of high density cultures of astrocytes surrounding devices demonstrated that cell distribution

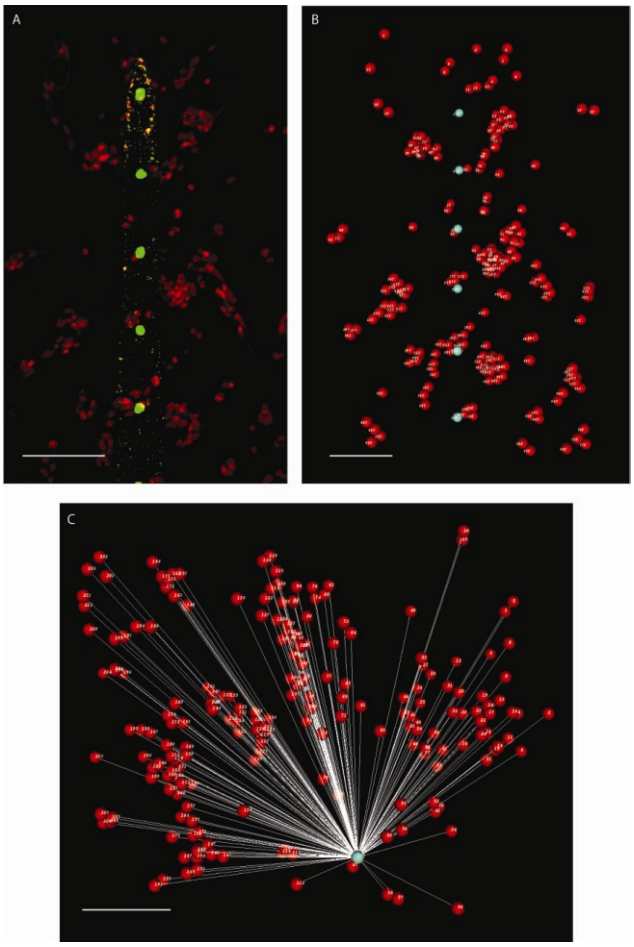

Fig. 2. Automated image analysis and mapping can be used to describe the distribution of glial cells around neuroprosthetic devices *in vitro*. (A) Confocal images were collected from cultures of glial cells surrounding microfabricated neural probes. This image shows a culture of astrocytes labeled with the nuclear stain Hoechst 33342. Electrode and probe location were determined from autofluorescence and reflected signals. (B) FARSIGHT software was used to segment and measure the distribution of cells within the 3-D confocal image volumes. A rendered image of (A) is shown with red spheres indicating the location of cells and green spheres indicating the location of electrodes. (C) A 3-D rendering and distance map from image (B) is presented to illustrate the spatial relationships between one electrode and the cells within the 3-D construct. Scale bars =100 μm.

could be mapped in 3-D space surrounding electrodes (Fig. 2A-C). Distance maps generated from the physical addresses of cells and electrodes within confocal image volumes demonstrated that astrocytes surrounded device electrodes in a radial pattern. These data are being used to associate impedance changes with cell distributions.

IV. Discussion

A method has been described for impedance measurement, analysis and histological correlation for bare electrodes and electrodes surrounded by cell-seeded alginate 3-D brain constructs. The results from impedance characterization and EIS data modeling confirm that EIS can be used to quantify the electrical properties of electrodes and tissues with minimal disruption to the sample under investigation. The sensitivity, stability and reproducibility of the impedance measurements permit accurate analysis over several time points and could potentially be used to record time lapse impedance data. The ability to model data using standard fitting algorithms adapted for use with equivalent circuit parameters provides a method to describe the physical basis of EIS data.

The circuit elements described in this report can be separated into two groups; elements that can be attributed to the electrode and electrode/solution interface (R_{sol}, R_{ct} and CPE) and elements that can be attributed to the cell construct coating material (C_{cells} and $Z_{Warburg}$). The circuit elements used to model the cellular contributions to impedance were selected based on the known capacitive properties of lipid bilayers (C_{Cells}) and the observed reduction in extracellular space in high density cell scaffolds that can affect the diffusion of chemical species ($Z_{Warburg}$) [2, 8, 13, 15, 3]. The Warburg impedance has been used to model a variety of other types of electrical coatings of up to 100 μm in thickness with pore sizes on the order of 20 μm [18, 22]. It could be possible to improve the fit slightly by adding additional circuit elements. However, it was found that additional elements did not reduce the χ^2 value (goodness of fit) enough to justify the additions (a decrease of 1 order of magnitude required per additional element). Therefore the following model is proposed. Cell constructs contribute additional impedance in two ways (i) by contributing capacitance in the form of plasma membrane lipid bilayers (transcellular current pathway), and (ii) by reducing the amount of free space for chemical species and electrical current to flow, resulting in a Warburg impedance (extracellular current pathway).

The ability to use automated image analysis and feature mapping provides a valuable tool for correlating the modeled impedance changes with changes in cell distribution around the electrodes. This measurement system will be useful for monitoring the changes in impedance that accompany glial response to neuroprosthetic devices and can also be applied for use in a variety of biosensor applications. By applying models, such as the one described in this report, it is possible to interpret impedance data in terms of the changes that occur in tissue composition and structure.

References

[1] Banker G a G, K. 1998 *Culturing Nerve Cells* (Cambridge: MIT Press)

[2] Bard A J, and Faulkner, L.R. 2001 *Electrochemical Methods: Fundamentals and Applications* (New York: John Wiley & Sons)

[3] Bertrand C A, Durand D M, Saidel G M, Laboisse C and Hopfer U 1998 System for dynamic measurements of membrane capacitance in intact epithelial monolayers *Biophys J* **75** 2743-56

[4] Bjornsson C S, Lin G, Al-Kofahi Y, Narayanaswamy A, Smith K L, Shain W and Roysam B 2008 Associative image analysis: a method for automated quantification of 3D multi-parameter images of brain tissue *J Neurosci Methods* **170** 165-78

[5] Crone C and Olesen S P 1982 Electrical resistance of brain microvascular endothelium *Brain Res* **241** 49-55

[6] Frampton J P, Hynd M R, Williams J C, Shuler M L and Shain W 2007 Three-dimensional hydrogel cultures for modeling changes in tissue impedance around microfabricated neural probes *J Neural Eng* **4** 399-409

[7] Franks W, Schenker I, Schmutz P and Hierlemann A 2005 Impedance characterization and modeling of electrodes for biomedical applications *IEEE Trans Biomed Eng* **52** 1295-302

[8] Gamry 2007 Basics of Electrochemical Impedance Spectroscopy. In: *Application Note,* (Warminster: Gamry Instruments)

[9] Giaever I and Keese C R 1993 A morphological biosensor for mammalian cells *Nature* **366** 591-2

[10] Heroux P and Bourdages M 1994 Monitoring living tissues by electrical impedance spectroscopy *Ann Biomed Eng* **22** 328-37

[11] Linderholm P, Braschler T, Vannod J, Barrandon Y, Brouard M and Renaud P 2006 Two-dimensional impedance imaging of cell migration and epithelial stratification *Lab Chip* **6** 1155-62

[12] Liu X, McCreery D B, Carter R R, Bullara L A, Yuen T G and Agnew W F 1999 Stability of the interface between neural tissue and chronically implanted intracortical microelectrodes *IEEE Trans Rehabil Eng* **7** 315-26

[13] Macdonald J R 1987 *Impedance Spectroscopy: Emphasizing Solid Materials and Systems* (New York: John Wiley & Sons)

[14] McAdams E T, Jossinet J, Subramanian R and McCauley R G 2006 Characterization of gold electrodes in phosphate buffered saline solution by impedance and noise measurements for biological applications *Conf Proc IEEE Eng Med Biol Soc* **1** 4594-7

[15] Muralidharan V S 1997 Warburg impedance –basics revisited *Anti-Corrosion Methods and Materials* **44** 26–9

[16] Rahman A, Lo C and Bhansali S 2008 A Detailed Model for High Frequency Impedance Characterization of Ovarian Cancer Epithelial Cell Layer Using ECIS Electrodes *IEEE Trans Biomed Eng* **56** 485-492

[17] Ribaut C, Reybier K, Reynes O, Launay J, Valentin A, Fabre P L and Nepveu F 2008 Electrochemical impedance spectroscopy to study physiological changes affecting the red blood cell after invasion by malaria parasites *Biosens Bioelectron* **24** 2721-5

[18] Savitri D and Mitra C K 1999 Modeling the surface phenomena in carbon paste electrodes by low frequency impedance and double-layer capacitance measurements *Bioelectrochem Bioenerg* **48** 163-9

[19] Suner S, Fellows M R, Vargas-Irwin C, Nakata G K and Donoghue J P 2005 Reliability of signals from a chronically implanted, silicon-based electrode array in non-human primate primary motor cortex *IEEE Trans Neural Syst Rehabil Eng* **13** 524-41

[20] Szarowski D H, Andersen M D, Retterer S, Spence A J, Isaacson M, Craighead H G, Turner J N and Shain W 2003 Brain responses to micro-machined silicon devices *Brain Res* **983** 23-35

[21] Varlan A R and Sansen W 1996 Characterisation of planar electrodes realised in planar microelectronic technology *Med Biol Eng Comput* **34** 308-12

[22] Wang B, Luo J, Wang X, Wang H and Hou J G 2004 Dielectric properties and frequency response of self-assembled monolayers of alkanethiols *Langmuir* **20** 5007-12

[23] Weiland J D, Anderson D J and Humayun M S 2002 In vitro electrical properties for iridium oxide versus titanium nitride stimulating electrodes *IEEE Trans Biomed Eng* **49** 1574-9

[24] Williams J C, Hippensteel J A, Dilgen J, Shain W and Kipke D R 2007 Complex impedance spectroscopy for monitoring tissue responses to inserted neural implants *J Neural Eng* **4** 410-23